

ABSTRACT

Title of thesis: DEVELOPMENT OF A TURBULENT
WOLFHARD-PARKER BURNER WITH
SUPPRESSING CO-FLOW

Eric D. Link, Master of Science, 2014

Thesis directed by: Associate Professor André Marshall
Department of Fire Protection Engineering

A burner and surrounding co-flow air system were developed for experimental study of flame suppression in a diluted oxygen environment. Development of the burner was guided by design criteria requiring the flame to be a turbulent buoyant diffusion flame in a line configuration presenting a realistic challenge to suppression methods such as oxidizer-stream dilution. Design constraints included buoyancy, turbulence, and flame height criteria. Oxygen concentration and temperature measurements, along with a smoke wire flow visualization technique were utilized to evaluate the system and ensure the design criteria were successfully met. Additional analysis was performed on image recordings of the flame to provide a robust and repeatable flame height measurement to evaluate the flame height constraint. Ultimately, an experimental apparatus with the ability to suppress a flame in a controlled, well-characterized environment was developed to provide a good base for model validation measurements.

DEVELOPMENT OF A TURBULENT WOLFHARD-PARKER
BURNER WITH SUPPRESSING CO-FLOW

by

Eric D. Link

Thesis submitted to the Faculty of the Graduate School of the
University of Maryland, College Park in partial fulfillment
of the requirements for the degree of
Master of Science
2014

Advisory Committee:

Associate Professor André Marshall, Chair/Advisor

Assistant Professor Michael Gollner

Professor Arnaud Trouvé

© Copyright by
Eric D. Link
2014

Acknowledgments

This work is in support of a larger research project collaboration between the Department of Fire Protection Engineering at the University of Maryland, FM Global, and United Technologies Research Center. This research would not be possible without the support of the industry sponsors, both financially, and with their guidance in weekly update meetings. I am also thankful for additional funding provided by the National Science Foundation (Award #1236788).

I would like to thank the the professors, students, interns, and industry partners who were involved with the GOALI team for their help along the way to make this possible. Special thanks go to my fellow student, James White, who was instrumental in the success of this project and provided help and guidance along the way. Further, I would like to thank Dr. André Marshall for his support as my advisor and PI, as well as Dr. Peter Sunderland and Dr. Arnaud Trouvé, who were continuously involved as co-PI's throughout the project. Thanks also to Dr. Michael Gollner, for support and participation in my thesis committee. Finally, I would like to thank UTRC for their help with the fabrication of the final burner.

Table of Contents

List of Tables	v
List of Figures	vi
1 Introduction	1
1.1 Overview	1
1.2 Literature Review	2
1.2.1 Lab Burners	3
1.2.2 Flame Height	6
1.3 Objective	9
2 Approach	10
2.1 Design Concept	10
2.2 Apparatus Construction	13
2.2.1 Burner Details	13
2.2.1.1 Burner Prototypes	14
2.2.1.2 Final Burner	15
2.2.2 Co-Flow Details	17
2.2.3 Additional Design Findings	21
2.3 Inlet Characterization Diagnostics	24
2.3.1 Oxygen	24
2.3.2 Smoke Wire	25
2.4 Flame Characterization Diagnostics	27
2.4.1 Temperature	27
2.4.2 Flame Height	30
2.4.3 Alternate Flame Height Method	35
3 Results	37
3.1 Inlet Measurements	37
3.1.1 Flow Rate	37
3.1.2 Smoke Wire	38
3.1.3 Oxygen Concentration	40

3.2	Flame Measurements	41
3.2.1	Temperature Profiles	41
3.2.2	Flame Height	43
3.3	Suppression Ability	45
4	Conclusions and Future Work	46
	Bibliography	48

List of Tables

2.1	Burner design criteria	12
3.1	Flame height measurements	45

List of Figures

2.1	Design concept	13
2.2	Burner design drawing	16
2.3	Co-flow design drawing	18
2.4	Co-flow components	19
2.5	Co-flow blockage effect	22
2.6	Oxygen anchor schematic	23
2.7	Smoke wire configuration	26
2.8	Thermocouple array	28
2.9	Temperature measurement	29
2.10	Flame height measurement dependence on sample size	31
2.11	Converting RGB image to binary image	32
2.12	Flame height image	34
2.13	Alternate flame height measurement	36
3.1	Smoke wire image	39
3.2	Smoke-wire velocity estimate	40
3.3	Temperature profile	42
3.4	Alternate flame height method results	44
3.5	Flame suppression	46

Chapter 1: Introduction

1.1 Overview

Computer modeling and CFD codes are utilized increasingly for performance-based fire protection engineering applications. One limitation of current CFD codes is accurate modeling of complex suppression phenomena. In the interest of providing experimental data relevant to model development and validation, a well characterized and controlled flame apparatus with a suppression ability is desired. Numerous suppression studies have been conducted with various fuels and suppressing agents, primarily for laminar flames in small-scale configurations. To expand the existing data sets, and to provide new data for turbulent flames more consistent with accidental fires, a turbulent flame suppression apparatus is needed. Additionally, a well-controlled and characterized system is important to provide useful information for incorporation into, and validation of, CFD models.

The development of this experimental apparatus is a portion of a larger research endeavor focused on providing experimental support to computer modeling validation efforts in the area of fire-spray interactions and suppression of fires with water spray or mist. The overall project consists of experiments to investigate three areas of fire suppression—spray transport, spray-flame interaction, and spray-

radiation interaction. The design of this experimental apparatus will support efforts relating to the spray-flame interaction aspect including flame extinction and radiation impacts of water mist.

To this end, this work details the development of a Wolfhard-Parker slot burner with a surrounding co-flow, capable of producing a turbulent diffusion flame in a well-characterized environment, for investigation of fire suppression mechanisms. The design requires that the burner produce a buoyancy dominated turbulent diffusion flame with minimal soot production in a line-fire configuration. Additionally, the flame must exist in a well-controlled co-flowing environment which will serve two purposes; the co-flow will isolate the flame from ambient room disturbances, and deliver the suppressing agent to the flame region with low momentum to avoid flame penetration effects. Measurements and diagnostics, including oxygen concentration measurements, a smoke-wire flow visualization, and a computerized flame height calculation derived from images of the flame were used to evaluate the performance of the experimental apparatus.

1.2 Literature Review

A review of previous experimental apparatuses presented no burner that could produce the desired flame behavior for the future suppression studies. Absent from the literature is a study of medium-scale turbulent flame suppression in a controlled environment. Suppression studies have primarily been conducted on small-scale, bench-top, laminar flames. Literature about burners used in prior suppression

studies, as well as rectangular line-type burners, was helpful in the design of this Wolfhard-Parker slot burner.

The desire for a burner with a line fire configuration would require a diagnostic to evaluate the behavior of the flame, namely the flame height. In defining a line fire, one of the criteria is that the flame height be less than 10 times the short dimension of the burner. Having a reliable flame height measurement is important to evaluate this criterion. However, there are multiple definitions of flame height as well as several methods that have been used to measure it in the past.

1.2.1 Lab Burners

Previous bench- and laboratory-scale experiments investigating suppression of diffusion flames have used several different types of burner geometries in both counter-flow and co-flow configurations, and used gas suppression agents such as nitrogen, carbon dioxide, argon, helium, and halon [1–9], or water-mist [4, 6, 9–11].

Counter-flow burners introduce the fuel and oxidizer in opposite directions, and the flame stabilizes at the stagnation point of the two streams. The suppressing agent is introduced in either the oxidizer air stream or in the volume surrounding the combustion location. Various designs exist, such as those by Simmons and Wolfhard [1] and Tsuji [3, 7, 12], where the fuel is introduced by small porous burners suspended in the air stream. The Simmons and Wolfhard [1] configuration consists of a small hemispherical stainless steel burner situated in the center of an upward air stream contained by a glass cylinder. Fuel is continually supplied to the burner

in the downward direction, and the flame is sustained a few millimeters from the burner surface. A similar type of burner was made by Tsuji [3, 12] and consists of a small porous cylinder oriented horizontally in an air stream chamber. The fuel is supplied through the cylinder and produces a laminar flame at the stagnation point where the air flow meets the bottom of the cylinder. The inert gas diluent can then be added to the air stream to study flame suppression.

A different design approach was taken by Puri and Seshadri [8], who designed an apparatus to introduce the fuel and oxidizer streams in opposite directions directly from supply ducting rather than supplying the fuel to a burner. In this configuration, a steady flame disk was stabilized between the two counter flowing streams. Diluent can be added to both the fuel or oxidizer streams. The configurations used by Suh [4], Atreya [10], and Lazzarini [11] used a similar design, but added water mist or vapor to the air stream [4] or surrounding air volume [10, 11].

Co-flowing configurations supply the oxidizer and suppressing agent in the same direction as the fuel flow from an opening surrounding the flame. Co-flowing burner configurations used for suppression studies have included the cup burner [2, 5, 6] and the Santoro burner [7], along with a modified Wolfhard-Parker slot burner [9].

The cup burner was developed in 1977 to improve on the experiments done by Simmons by reducing the burner effects and eddies created by the edges of the burner [2]. The design is detailed in the appendix of the NFPA 2001 standard [13], which provides code guidance on fire suppression using clean agents. A cup of fuel is positioned in the center of a co-flowing oxidizer stream contained inside a glass

chimney. The tapered shape of the cup smooths the air flow around the burner so that a very stable laminar flame can be sustained. Suppression agents are introduced to the flame by addition to the oxidizer stream. Water mist has also been utilized as a suppressant in the cup burner configuration [6]. In the water mist case, the mist was generated inside the chimney upstream of the burner cup. The air stream with water mist droplets then passed through a series of wire screens before interacting with the flame.

A co-flow diffusion burner, developed by Santoro [14] to study laminar flames, has also been used to study flame suppression [7]. In this burner configuration, the flame is stabilized above a small circular fuel tube and is surrounded by an annular co-flow port that provides a slow flow of air. In the case of the suppression studies by Pitts [7], the suppressing agent was added to the air stream.

In a smaller-scale study similar to those planned using the current burner, Ndubizu et al. [9] designed a Wolfhard-Parker type slot burner with co-flow openings on either side of the burner. Their study explored the mechanisms of water mist fire suppression on small-scale two-dimensional flames. The burner they developed was 75 mm long by 10 mm wide and had a depth of 150 mm. Methane fuel was supplied from the bottom of the burner which was filled with fine sand to generate a uniform fuel supply on the surface of the burner. Various suppressants, including nitrogen, steam, and water mist, were introduced to the flame via a co-flow system that was 82 mm long and 35 mm wide, positioned along both long sides of the burner. Water mist was generated in mixing chambers that were connected to the co-flow streams. With fuel supplied at 2.81 cm/s, the approximate heat release rate of their burner

was 0.7 kW.

Line burners developed by Hasemi and Nishihata [15] had adjustable aspect ratios to investigate shape effects of the fuel on flame height. The burner could be arranged to provide dimensions ranging from 0.2×0.2 m to 0.2×1 m. A separate burner with aspect ratio of 10:1 was also constructed having dimensions of 0.1×1 m. Burners were filled with ceramic beads to distribute the fuel across the burner surface. Their experiments suggest that burners with length-to-width aspect ratios of 10:1 approach the behavior of line-plumes. Their data also suggests that with a 10:1 aspect ratio and a 50 kW fire, the flame height, defined as the observed mean flame-tip height, will be approximately 0.5 m.

1.2.2 Flame Height

Flame height is a basic integral measurement of fire size and behavior that is commonly measured, and can be compared to correlations or computer model simulations. Flame height has been used as a metric related to fire size, as it is generally easier to measure compared to heat release rate. Flame height is also a relatable quantity in terms of getting a mental picture of fire size. In the case of accidental fires, or any fire outside of a laboratory environment, the heat release rate is likely unknown, and a correlation with flame height provides an engineering estimate of the fire size. However, an important note is that there are a few definitions of flame height that are commonly used by reviewing video recordings of the flame. A simple, yet more subjective measurement, can be made by observing the flame tips and

visually averaging the height over time [15–17]. This method can depend on the judgement of the observer. A more robust method utilizes quantitative analysis of the video to repeatably define a mean flame height based on the intermittency of the flame [18–20].

A list summarizing various flame height correlations developed is presented by Beyler [21], however this list only includes one experimental correlation developed from line-fire configurations; much of the work has been done relating to pool fires with round or near-square fuel geometries. The various correlations indicate that the flame height becomes dependent on fuel geometry, i.e. the diameter, for shorter flames. Hasemi and Nishihata [15] later conducted experiments on various fuel shapes, ranging from a square burner to a line burner, with a length-to-width aspect ratio of 10:1, to evaluate the shape effects. More recently, Grove and Quintiere [22] published correlations for flame height and entrainment rates for infinite line fire sources based on line plume theory and data from several existing studies.

Flame height of large turbulent flames presents multiple challenges compared to the same measurement for laminar flames. Unlike a steady laminar flame, fluctuations of turbulent flames in both time and space require a mean flame height measure. Prior to more precise and robust techniques, flame height was measured using visual estimates by observers. Zukoski [18] incorporated video recordings of the flame to develop a more robust definition by which to measure the flame height. Using this method, the flame is represented by the visibly radiating portion of the plume. On the recorded images, the visible flame has high contrast with the surroundings, and thus the flame is easily identified. The recorded images can be

analyzed to determine the fluctuations in the flame location, or the intermittency of the flame at a given height. The mean intermittent flame height is defined as the height at which the flame intermittency is 0.5—meaning a portion of the flame exists above that height 50% of the time. Results of this method show that visual estimates of the flame height lie 10-15% higher than the 50% intermittent flame height.

Audouin et al. [19] employed this definition of flame height for experiments of pool fires and measured both the mean flame height and the intermittent flame region of the plume with different intermittency criteria. The Zukoski method of watching flame tip height was expanded by evaluating a series of images capturing the entire flame over time. Images were examined to determine the flame position and converted from their original colored version to a grayscale image with intensity values ranging from 0 (black) to 255 (white). The grayscale images were then converted to binary versions, where intensity values greater than 110 were indicative of flame presence and reassigned a value of 1. The lower values were assigned a value of 0, indicating the flame was not at that position. Averaging a sequence of 160 random frames from a video recording produced a map of characteristic flame shapes and the probability of the flame existing at any location. Using the Zukoski 50% intermittent definition of mean flame height, the points in the image with intensity values of 0.5 were averaged to determine the flame height.

Experiments done by Hasemi and Nishihata [15] used propane fuel, and flame height was measured by observing the height of the flame tips for 3 minutes. The authors found that for large heat release rates, the aspect ratios studied did not

have a large influence on the flame height and the behavior was dominated by the relation of square fuels, scaling like $Q^{2/5}$. However, with low enough heat release rates, the fuel shape is an influential factor, and rectangular fuels approach the line fire scaling of $Q^{2/3}$. This critical heat release rate limit for line fires was found to be 100 kW for the 0.1 m×1.0 m burner.

1.3 Objective

The burner apparatuses previously used do not provide the desired size or flame characteristics for the planned suppression studies; they produce small-scale, generally laminar flames. To study the suppression of a turbulent fire comparable to accidental fires, in a configuration to make detailed measurements possible, a new laboratory-scale burner with a suppressing co-flow apparatus is desired. Therefore, the objective of this work is to develop such a facility. Several design criteria must be met to remain consistent with a turbulent, buoyant, diffusion flame in a line-fire configuration. The co-flowing air/suppression supply must be able to challenge the flame such that suppression can be achieved. Finally, the system must be well-characterized to yield useful computer model inputs for model validation. As part of a team research endeavor, the scope of this work is to design and fabricate the physical experimental apparatus according to previously determined design goals and specifications [23]. Furthermore, this work includes diagnostics and measurements to evaluate the success of the experimental apparatus with respect to the

various design criteria.

Chapter 2: Approach

Initially, a set of design requirements relating to the flame and co-flow characteristics were determined [23], and will be discussed in following section. The design of an experimental apparatus to meet the requirements began with a general design concept similar to the smaller-scale study performed by Ndubizu [9], where a rectangular slot burner was surrounded by a co-flowing air and suppression delivery port. Design of the burner was mostly completed before the co-flow to determine the flame characteristics and dimensions the co-flow would need to accommodate. After the two systems were combined, various diagnostics were used to evaluate the performance of the system in relation to the original design requirements.

2.1 Design Concept

The design of the burner system was guided by the desired flame characteristics and the ability to suppress the flame with inert gas diluent added to the oxidizer stream. Design goals included a turbulent, buoyancy dominated, two-dimensional line fire with minimal soot production. These criteria are important so the burner produces a well-characterized flame with which to study suppression. Design parameters used to achieve these goals include the burner dimensions, fuel type, and

fuel flow rate. The development of the design criteria are briefly discussed here, and are further detailed by White [23].

The flame turbulence is gauged by a flame Grashof number, Gr , defined as

$$Gr = \frac{g\beta(\dot{Q}/L_b)x^3}{\rho_\infty c_p \nu_\infty^3} \quad (2.1)$$

where g is gravitational acceleration, β is the coefficient of thermal expansion, \dot{Q} is the heat release rate, L_b is the length of the burner, x is the vertical distance from the source, ρ_∞ is the ambient air density, c_p is the specific heat of ambient air, and ν_∞ is the kinematic viscosity of ambient air. To ensure the flame is predominately turbulent, the Grashof number must exceed a critical value a short height above the surface of the burner. As a conservative value, a Gr of 10^{11} was desired at a distance one tenth the flame height.

The buoyancy constraint is evaluated using a dimensionless energy release rate, Q^* , representative of a Froude number [15, 20], determined as

$$Q^* = \frac{\dot{Q}/L_b}{\rho_\infty c_p T_\infty \sqrt{g} w_b^{3/2}} \quad (2.2)$$

where T_∞ is the air temperature, and w_b is the width of the burner. This metric is constrained to be less than 10 to maintain a buoyancy dominated source in order to be consistent with typical accidental fires and to be well removed from the jet source region at high values of Q^* .

The final flame constraint is to maintain a two-dimensional line fire, requiring that the flame height be less than the length of the burner and also that the burner is at least 10 times longer than its width.

An additional design constraint is applied to the co-flow air supply. To avoid influencing the characteristic flame shape and behavior, the velocity of the supplied co-flowing air, u_c , should be much less than the buoyant velocity generated in the flame, u_f . Constraining the velocity of the co-flow to one tenth of the buoyant flame velocity, this objective can be met. The various dimensionless design criteria are compiled in Table 2.1.

Table 2.1: Dimensionless burner design criteria

Design Objective	Constraint
Turbulent	$Gr > 10^{11}$
Buoyant	$Q^* < 10$
Two-dimensional	$L_f/L_b < 1$
	$L_b/w_b > 10$
Co-flow	$u_f/u_c > 10$

Design of the co-flow portion of the apparatus was guided by the goal to provide a well-characterized environment for the flame without influencing the flame behavior. To control the flame environment, care must be taken to provide sufficient co-flow air to prevent ambient room air from interacting with the flame. However, supplying air in a co-flow arrangement has the possibility of modifying the flame behavior by forcing an air supply rather than allowing natural air entrainment. For example, the flame could be lengthened or could lift-off from the burner if the velocity of the co-flow is too high. The goal of achieving the desired air supply without altering the flame with a high-velocity air supply aided in the sizing of the co-flow. By using a larger flow area, a lower air velocity is required for the same volumetric flow rate.

2.2 Apparatus Construction

The experimental system consists of the Wolfhard-Parker slot burner and co-flow air/diluent supply systems. This section provides descriptions and details of the different components. The apparatus incorporates a rectangular slot burner, centered in a co-flowing air supply, in order to produce a turbulent line fire as shown in Fig. 2.1. A sufficient amount of air to shield the flame from the ambient room and to allow complete combustion would flow parallel to the flame. Gas diluent, added to the air supply, would provide the means of flame suppression.

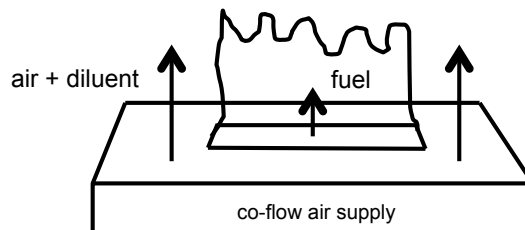


Figure 2.1: A rectangular shaped slot burner centered in a surrounding air supply was the original concept of the system. Diluent added to the air supply will challenge the flame toward suppression.

2.2.1 Burner Details

Design of the burner was completed prior to the co-flow system. Initial attempts at burner sizing and fabrication were performed in the lab using sheet metal to determine the appropriate dimensions and fuel supply details. After developing a design that tentatively met the requirements, fabrication of a higher quality burner

was completed using welded stainless steel. Various diagnostics and measurements were performed to characterize the final burner.

2.2.1.1 Burner Prototypes

A series of prototype burners was fabricated during the design process. The first burner was built with a length of 24.5 cm and width of 4.5 cm using 0.91 mm (0.036 in.) thick galvanized steel sheet metal. This prototype was 5.6 cm deep and was filled completely with sand. The sand used for the duration of this work was Sakrete brand medium coarse multi-purpose sand, additionally filtered using an 18×18 wire mesh of 0.22 mm diameter wire with 1.2 mm openings (0.009 in. wire and 0.047 in.) to remove coarser sand particles. The fuel was supplied through a single inlet port at the midpoint of the burner. Testing showed this burner produced a triangular shaped flame and thus did not satisfy the line fire design criteria.

A more uniform fuel flow rate at the surface of the burner was required to improve the shape of the flame. The pressure drop along the axis of the burner had to be reduced so that the pressure drop in the vertical direction was greater than that along the axis of the burner. This way the fuel uniformly fills the length of the burner before reaching the surface. One possible method to increase the pressure drop was to increase the depth of the sand. However, this would require a higher operating pressure leading to fluidization of the sand bed. The similar burner used by Ndubizu [9] had a sand depth twice the length of the burner, which would be a significant depth for the current burner. A second method was to introduce the fuel

to an empty plenum space before flowing through the sand bed. This maintains a lower operating pressure and also reduces the size of the burner compared to one full of sand. After modifying the original prototype to include a plenum space, the flame shape was improved, however the flame did not display the desired turbulence. The short burner configuration required a heat release rate that was too large relative to the shape of the burner to reach the desired turbulence level, and did not meet the line-fire configuration criteria.

Using the same plenum and porous sand bed design, a second burner was fabricated with an increased length-to-width aspect ratio of 10:1 in an effort to better meet the line geometry constraint. Testing with liquid saturated Kaowool insulation wicks of various sizes indicated this aspect ratio produced stable line fire behavior. The 10:1 aspect ratio is also suggested by Hasemi and Nishihata [15] as approaching a line fire configuration. The dimensions of the new prototype were 5 cm wide by 50 cm long. Testing of this burner showed a successful design with respect to flame shape, height and turbulence.

2.2.1.2 Final Burner

After the observations and experience gained from the prototype burners, a final burner was fabricated as diagrammed in Fig. 2.2. The burner is constructed from stainless steel with dimensions 5 cm wide by 50 cm long, with a height of 7 cm. The burner consists of two sections—a 2 cm deep lower plenum section and a 5 cm deep porous upper section filled with sand to produce a pressure drop for uniform

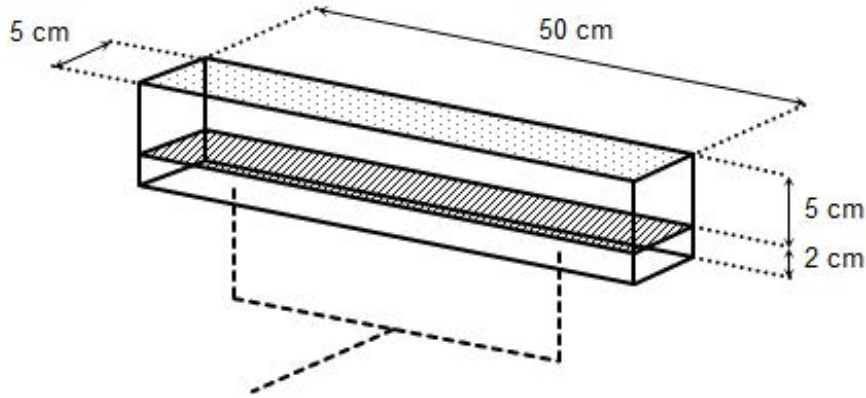


Figure 2.2: The burner is constructed of stainless steel and has a length of 50 cm and a width of 5 cm. The burner is 7 cm deep, consisting of a 2 cm deep empty plenum space covered by 5 cm of fine sand. There are two evenly spaced fuel injection points on the bottom.

flow. The sand is supported above the plenum using a rigid perforated steel plate and mesh screens to prevent sand from filling the plenum. To further distribute the fuel supply, two equally spaced fuel inlets, using 6.4 mm (0.25 in.) outer diameter tubes, were incorporated rather than the single inlet previously tested.

Methane (99.5% purity) is supplied from a compressed cylinder at a rate of 1.0 ± 0.02 g/s, corresponding to a 5.4 cm/s flow velocity from the burner surface, yielding an unsuppressed chemical heat release rate of 50 kW. Prior to flow measurement, the gas tubing passes through a water bath to supply the fuel at a constant temperature. The rotameter measurement was calibrated with an electronic mass flow controller and is adjusted for temperature and pressure. Testing of fuel flow rates was done qualitatively at first by observing the flame. A flow rate near 1 g/s was tentatively selected based on an estimated flame height and the flame turbulence. It was determined that an even flow rate to produce a fire source of 100 kW/m

was desirable, and falls in the acceptable line fire range determined by Hasemi and Nishihata. Later diagnostics confirmed that this flow rate was acceptable to meet all of the design requirements.

2.2.2 Co-Flow Details

The design of the co-flow surrounding the burner was developed with analysis from CFD to determine the amount of air flow required to isolate the flame from ambient room air [23]. By providing a well-characterized envelope for the flame, ambient movement in the room will not influence the flame, and the confidence in suppression measurements is increased because the flame is not interacting with more oxygen than provided by the co-flow. The CFD analysis indicated that an air supply of four times the stoichiometric oxygen requirement was sufficient to isolate the flame from the ambient environment. With this air flow, 90% of combustion products were produced by reactions with the co-flow air supply. Knowledge of the required air flow supply aided in the physical design of the co-flow. An important characteristic of the co-flow apparatus is that the air velocity is much less than the buoyancy induced flow in the flame to avoid altering the flame behavior. By knowing the amount of air required, the dimensions of the co-flow could be determined using a uniform co-flow velocity as an independent variable.

The co-flow box is constructed of wood in three stacked sections, sealed airtight, with inside dimensions measuring 75 cm long by 50 cm wide by 105 cm tall as shown in Fig. 2.3. The burner is supported by a column in the center, which also

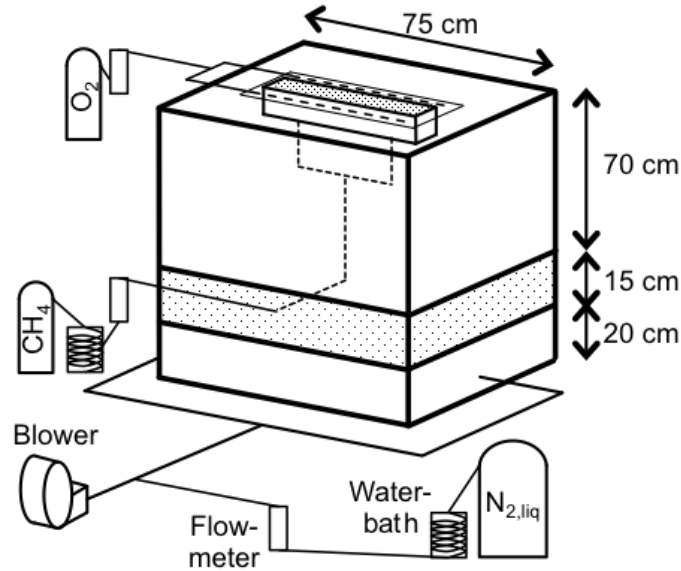


Figure 2.3: The co-flow is comprised of three sections: the bottom plenum space, the middle porous bed for flow mixing, and the top flow straightening section. The burner is supported in the center of the co-flow.

conceals the fuel supply tubing to prevent disturbance of the air flow. The sections are constructed separately and clamped together to facilitate any maintenance or potential internal adjustments required after construction. To produce a uniform flow distribution from the surface, the plenum technique used for the burner design was repeated. The bottom section is an empty plenum space where the air is introduced. It is 20 cm tall to accommodate the 7.62 cm (3 in.) PVC air supply pipes connected on either side of the box. In the 15 cm deep middle section is a porous bed of pea gravel that facilitates additional flow mixing and provides a uniformly distributed gas flow. The gravel is supported by a 3.2 mm (0.125 in.) thick perforated aluminum sheet. In addition to the gravel, this aluminum sheet supports the center pedestal that holds the burner. The internal components are shown in Fig. 2.4. On top, the

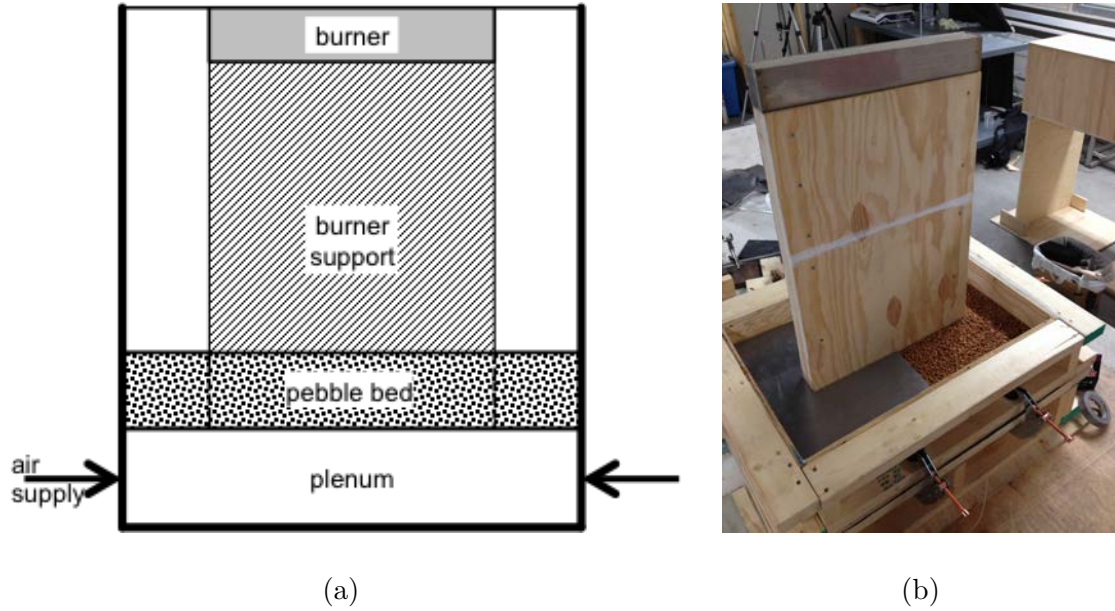


Figure 2.4: This schematic shows the inside of the co-flow and displays the various components including the pebble bed and center burner support. Fuel supply tubing is concealed inside the support. Below the pebble bed is the empty plenum space.

third section is empty other than a honeycomb flow-straightening piece at the top surface of the co-flow. The honeycomb is 3.8 cm (1.5 in.) thick and is constructed of aluminum tubes with 3.2 mm (0.125 in.) diameter, providing a length-to-diameter ratio of 12:1.

Air is supplied from a centrifugal blower at a maximum flow rate of 70 ± 10 g/s, equivalent to four times the stoichiometric requirement for the 50 kW methane flame. This base flow rate yields a co-flow velocity of 20 cm/s. Manual flow rate adjustment is possible using a gate valve located just downstream of the blower. Air flow was measured using a pitot tube connected to a differential pressure transducer (Setra Model 264). The pitot was located 2 m (81 in.) downstream of the gate valve, a

distance of 27 pipe diameters, to ensure the flow was fully developed and turbulent effects from the gate valve were avoided. A total pressure probe was inserted at the pipe centerline with an accompanying static pressure tap was located immediately downstream. The pressure transducer voltage output was calibrated to the system by measuring the oxygen concentration in the co-flow while adding a known flow rate of nitrogen to the air stream.

Nitrogen gas was the inert diluent used to suppress the flame, and was added to the co-flow air stream prior to the co-flow assembly box. The nitrogen flow was introduced 0.53 m (21 in.), or 7 pipe diameters, downstream of the pressure measurement. The maximum flow rate nitrogen reached 50 ± 2.5 g/s, or 2400 L/min corresponding to an added 14 cm/s velocity at the co-flow surface, to produce varying levels of suppression. Due to the large flow rate of nitrogen required to achieve flame suppression, the gas was supplied from a liquid storage tank rather than conventional compressed gas cylinders. The dewar used in the current work had a liquid capacity of 240 L and a maximum tank pressure of 235 psi. Nitrogen was drawn from the gas valve on the tank, but to ensure that the nitrogen was in the gas phase and near room temperature, the supply tubing passed through a large water bath upstream of the flow measurement. Furthermore, the pressure-building capability of the nitrogen tank was used to maintain sufficient gas pressure in the tank for the duration of the experiment. The flow was controlled using a needle valve and measured using a rotameter before it was mixed to the room air supplied by the blower.

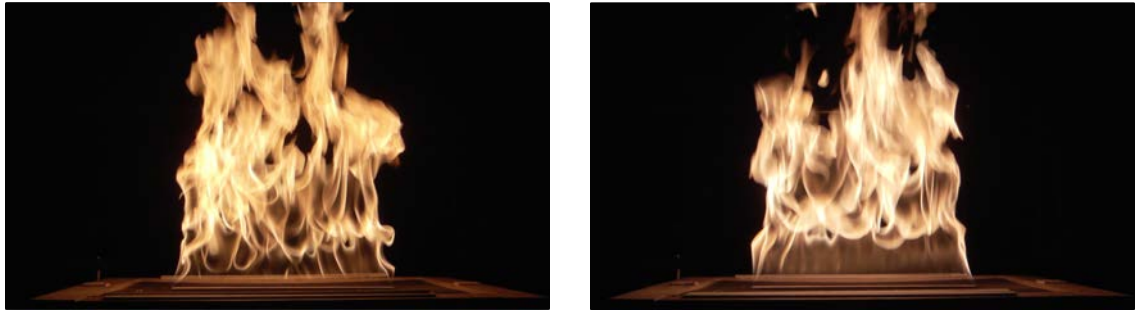
Downstream of the nitrogen introduction, a second 2 m length of pipe was installed before the flow was split two ways to be delivered symmetrically to the

box.

2.2.3 Additional Design Findings

During testing and experimentation with the completed assembly, several key observations were made leading to design improvements. Although the upper half of the flame displayed turbulent behavior, the parallel direction of the oxidizer stream exiting at the same surface of the burner induced an extended laminar region of the flame compared to the free-burning condition. The cause is believed to be from the oxidizer being provided in the streamwise direction, whereas the free-burning flame entrains oxidizer from a more cross-stream direction. To remove the initial laminar portion, the area of the co-flow opening within 5 cm of the burner edge was blocked using Kaowool insulation material to stimulate the turbulent behavior of the flame by adjusting the entrainment near the burner surface. The influence of the blockage is shown in Fig. 2.5. Note that Figs. 2.5a and 2.5c have similar turbulent behavior compared to the laminar portion of the flame evident in Fig. 2.5b.

During suppression events, it was observed that the primary extinction mechanism was due to flame base weakening followed by the flame lifting from the burner surface. This phenomena is consistent with previous observations in smaller diffusion flame configurations in reduced oxygen environments [2, 5, 7]. To prevent this flame lift-off extinction mechanism, a small flow of 99.994% pure oxygen was supplied directly to the flame base to improve the flame anchor to the burner. This was achieved by using sintered stainless steel tubes placed along each side of the



(a)

(b)



(c)

Figure 2.5: The effect of the Kaowool co-flow blockage is shown here: (a) Free-burn, no co-flow, (b) with co-flow, (c) with co-flow and blockage. Note the laminar flame base in case (b) where the co-flow influences the flame. By adding the blockage around the burner, the laminar portion was removed causing the flame to behave like the free-burning case.

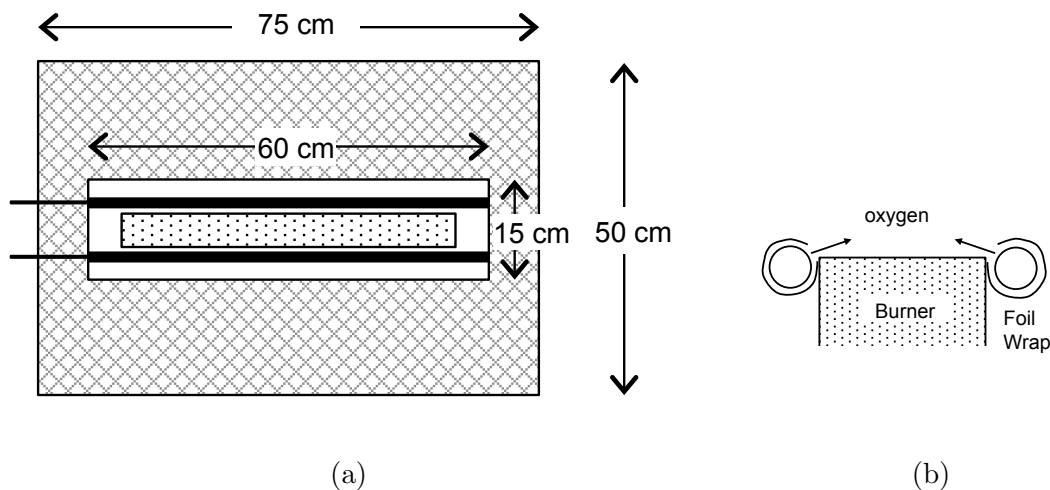


Figure 2.6: The porous oxygen anchor tubes were located along both sides of the burner, supported on the flow blockage (a). The tubes were wrapped with foil, except for an opening directing the gas directly to the flame (b).

burner, as shown in Fig. 2.6a. The tubes were 60 cm long and had an outer-diameter of 12.7 mm (0.5 in.). To deliver the oxygen directly to the flame, the tubes were wrapped tightly with aluminum foil such that gas could only flow through a narrow strip directed at a 45° angle toward the flame, depicted in Fig. 2.6b. Oxygen was supplied at a flow rate of 0.040 ± 0.0008 g/s (1.2 cm/s from the tube surface), which is expected to have a minimal impact on the reaction chemistry, as the flow rate is less than 1% of the oxygen required for stoichiometric combustion and less than 0.3% of the oxygen supplied by the co-flow.

It is also important to note that the uniformity of the sand in the burner is an important factor in flame behavior, particularly in low oxygen conditions. Uneven sand depths or coarse grained sand particles will influence flame behavior and could cause flame anchoring bias during extinction. To avoid these imperfec-

tions, the coarse particles were filtered out using a wire screen described in Section 2.2.1.1. Additionally, the surface of the sand was periodically re-leveled by scraping a straight-edge across the burner and adding more sand as needed.

2.3 Inlet Characterization Diagnostics

Several instrumentation and diagnostic techniques were utilized to evaluate the burner and co-flow system to determine if they successfully met the design requirements. In addition to the oxygen concentration measurements used for air flow calibration, two measurement diagnostics were implemented to evaluate the characteristics and uniformity of the co-flow environment that was developed around the flame. These included measurements of the spatial distribution of oxygen concentration at the co-flow surface and a flow visualization technique using a smoke-generating wire.

2.3.1 Oxygen

A paramagnetic oxygen analyzer (Servomex 540E) was used to measure the oxygen concentration of the co-flow supply at various locations to confirm that the air supply was well mixed and provided a uniform suppression environment. A sampling probe was placed at the co-flow outlet for a period of time to determine the steady-state oxygen concentration. Response and transport time of the gas analyzer was approximately 20 seconds, however the measurement was taken during steady-state conditions and is not affected by the time lag. Measurements were

taken at multiple locations at the opening of the co-flow box and indicate that the oxygen concentration at the co-flow outlet was uniform across the entire surface as desired.

2.3.2 Smoke Wire

To evaluate the uniformity of the velocity profile from the co-flow, a smoke generating wire technique similar to that done by Gaby [24] was used to visualize the flow field. A NiCr wire was strung across the opening of the co-flow and coated with mineral oil. An electric current supplied to the wire using a variable AC transformer caused the oil to generate a visible white smoke due to the heated wire. Video of the process was recorded and reviewed to provide visual confirmation of a uniform velocity profile.

The 2 m length of wire was suspended across the co-flow approximately 5.5 cm above the opening. On either side of the span, the wire was draped over non-conducting ceramic rods. Excess wire was wrapped around additional ceramic rods to maintain the resistance required to heat the wire. Weights attached to the ends of the wire maintained tension, as thermal expansion would otherwise cause the wire to lengthen and sag. This technique maintained a constant position of the wire for the duration of the test. The wire configuration is shown in Fig. 2.7.

It was determined that a continuous thin coating of oil applied to the wire by hand was the most effective application method. Placing individual drops along the wire did not work as well due to differences in drop size, uniform spacing, and

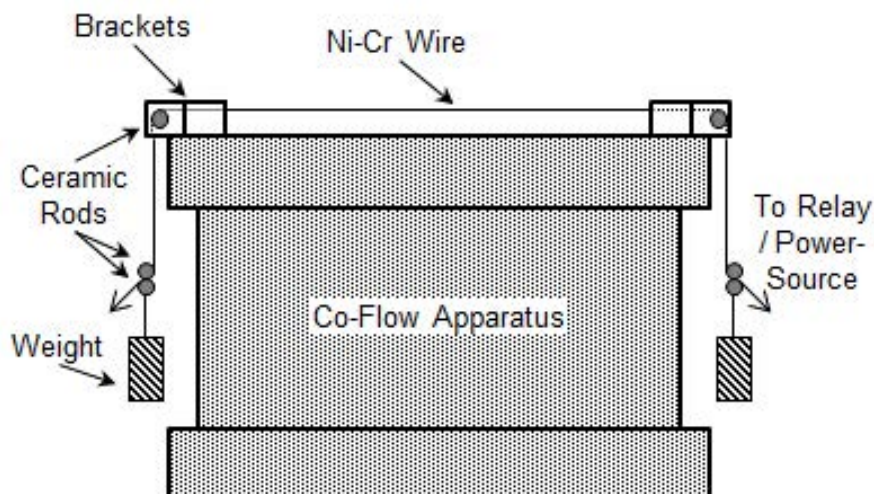


Figure 2.7: A 0.5 mm (0.02 in) diameter NiCr wire was suspended across the co-flow opening and coated with mineral oil. Weights were attached to either end of the wire to maintain tension when the wire increased in length when heated.

oil contact area with the wire. Although the smoke streaks were highly visible, it was difficult to reliably produce uniform streaks. By coating the entire wire, it was possible to produce a uniformly distributed line of smoke.

To provide repeatable experiments and consistent heating to the wire, a timing relay switch (SSAC TRDU24A3) was used to energize the wire for 0.2 s with 120 VAC. These parameters generated enough heat in the wire to produce visible smoke but not enough to cause significant turbulent flow structures in the smoke stream itself due to high buoyancy. By keeping the temperature to a minimum, the smoke more closely represents the flow pattern of the co-flow because it will have minimal induced momentum. Additionally, a quick pulse of smoke can be generated with a low heating time lag, important to tracking a distinct smoke front.

Videos of the experiments were analyzed primarily to visualize the uniformity

of the co-flow velocity profile. The uniformity of the smoke flow was judged qualitatively by watching the smoke front travel downstream. Estimation of the co-flow velocity was also attempted as a secondary metric from the video recordings. By tracking the position of the smoke front in the video, the velocity of the smoke can be estimated providing additional confirmation of the co-flow velocity as determined using the oxygen concentration measurements.

2.4 Flame Characterization Diagnostics

Temperature measurements and a flame height measurement from image analysis were conducted on the flame to confirm the vertical orientation of the flame and its behavior in the presence of the co-flowing oxidizer, and to evaluate its shape in relation to the desired two-dimensional line configuration.

2.4.1 Temperature

An array of 18 type-K thermocouples was used to measure the temperature profile of the flame perpendicular to the burner axis. Thermocouples were welded from 24 AWG, 0.511 mm diameter wire, and had bead diameters of 1 mm. These measurements were taken to provide additional confirmation that the co-flow was uniform and does not tilt the flame or affect the combustion in ways other than the desired suppression method.

The thermocouple wires were wrapped around and strung between two ceramic tubes, 6.4 mm (0.25 in.) in diameter, so the beads maintained a constant location

in the fluctuating flow. The wires were secured around the rod with binder clips. Thermocouple bead diameters were 1 mm and were spaced 1 cm apart near the flame (within 5 cm of the centerline), and 2 cm apart away from the flame as depicted in Fig. 2.8a. This spacing provided good resolution of the flame location near the peak of the profile. The actual device is shown in Fig. 2.8b.

A profile was a desirable configuration to be able to evaluate the symmetry of the flame and quantify any tilt that the ambient room geometry or co-flow may induce to the flame. However, due to the limited number of data channels available, half-profiles were measured, including 5 cm beyond the centerline to resolve the peak of the profile. This provided a sufficient number of data points to indicate the shape of the flame.

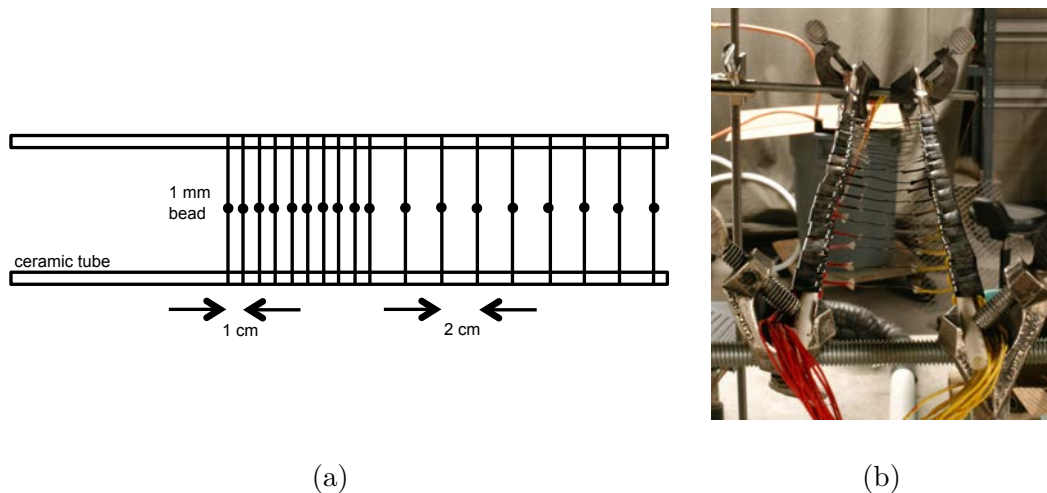


Figure 2.8: A probe containing 18 type-K thermocouples, with 1 mm bead diameters, was suspended perpendicular to the burner axis to measure temperature profiles at various heights to evaluate the flame. Beads were spaced 1 cm apart near the flame, and 2 cm apart further away (a). The actual device is shown in (b).

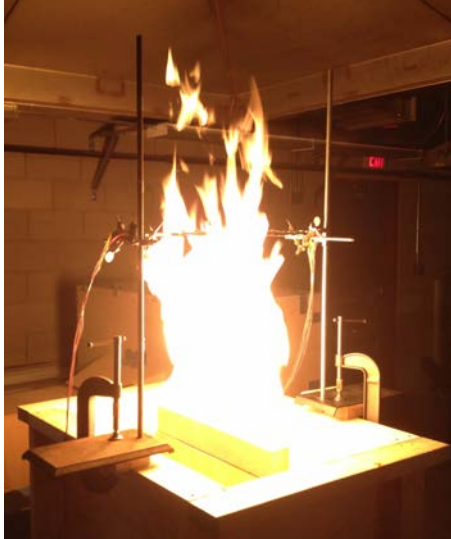


Figure 2.9: The thermocouple probe was positioned at various heights above the burner to measure time-averaged temperature profiles of the flame to indicate the flame position.

The flame and thermocouples were allowed time to reach a steady-state condition prior to the measurement period. Sampling was done at 1 Hz for a duration of 5 minutes to obtain time-averaged profiles. Due to the characteristics of the relatively large thermocouple beads, time-resolved measurements were not the intent of these measurements. Figure 2.9 shows the thermocouple probe in position across the flame. Care was taken to align the thermocouple with the centerline of the burner prior to each test using a plumb line to produce accurate profile shapes. Additional attention was given to the thermocouple beads to ensure that they were clear of soot at the beginning of each measurement period.

2.4.2 Flame Height

A robust flame height analysis method was developed to provide a consistent method to measure the visible height of the flame. Still images of the flame were captured and analyzed with a MATLAB script to determine the average visible flame height based on a 50% intermittent definition by Zukoski [18] and the technique of Audouin [19]. In the definition of Zukoski, the flame height is defined as the height both above and below which the flame exists 50% of the time. This location is determined through an image analysis routine that identifies the presence of the flame at each pixel in a series of photographs and calculates an average flame image that equates to an intermittency map.

A series of images are captured with the flame in a steady-state oxidizer condition using a Canon EOS 40D digital SLR camera. Images were captured for one minute at the nominal maximum continuous capture rate of 6 Hz. Care was taken that exposure settings were adjusted according to the flame brightness so there was a high contrast between the flame and the background. In the images used, contrast between the flame and the background was nominally 5, where contrast is defined as the intensity difference between the object and the background, normalized by the background intensity [25]. To ensure that a steady mean statistic was obtained, the variation of flame height measurement depending on the number of images used in the average was checked. The result shown in Fig. 2.10 indicates that the flame height measure becomes independent of the number of images if more than approximately 300 are used. Therefore, photos were recorded in sets of approximately 380

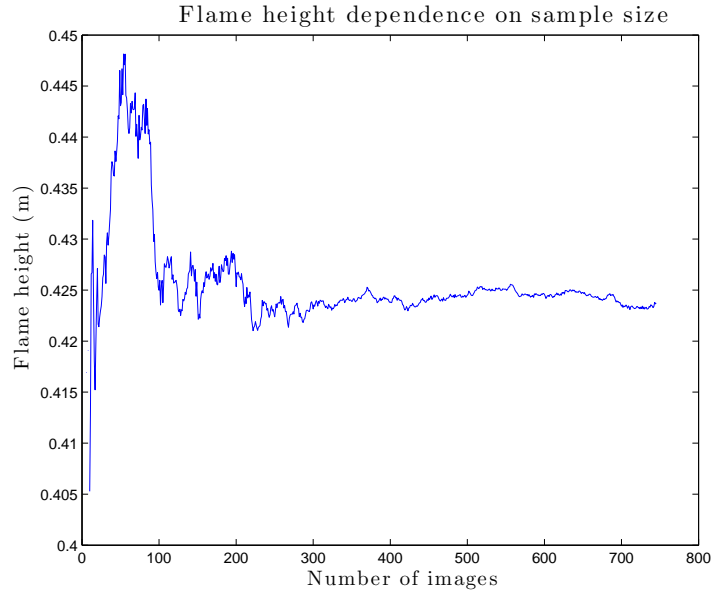


Figure 2.10: The mean flame height measurement is independent of the number of images used in the average calculation if the sample size is greater than about 300 images.

images. Each set was processed to determine the average flame height using the following procedure.

One photo from the set was used to determine the scale of the image frame using the known 50 cm length of the burner. This permits the conversion between number of pixels in the image to a physical length scale.

To determine the location of the flame on average, each image must be converted to a binary black and white image. After converting the original RGB color image to grayscale, a random selection of 5 images were manually converted to a binary copy by adjusting the threshold value. In the binary image, the flame is white while the remainder of the image is black. The mean value of the 5 random threshold values is used to convert all the images in the set. Manually selected

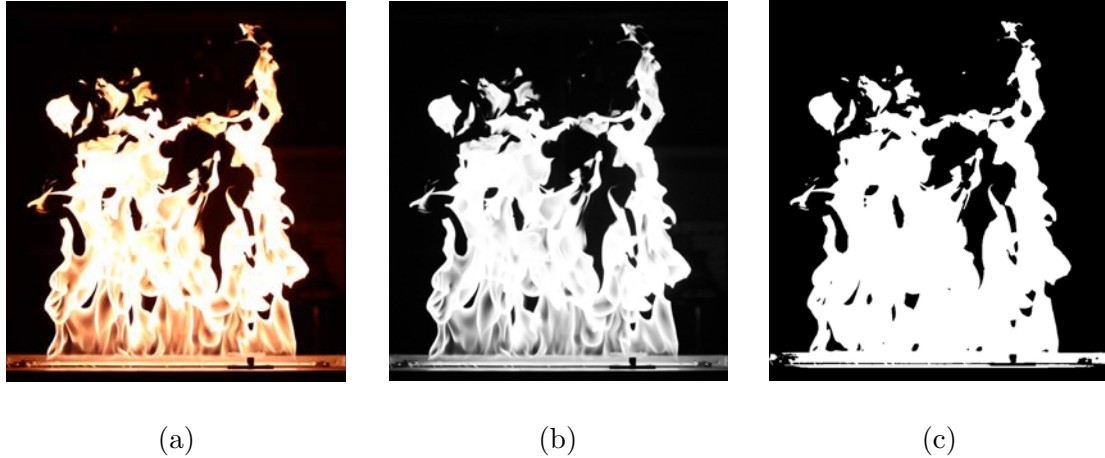


Figure 2.11: Each color RGB image (a) is first converted to a grayscale version (b). Then the image is converted to a binary image (c) with a threshold value that preserves the flame location.

threshold values do not vary significantly from image to image if the camera settings are constant. Manual selection of the threshold was preferred to automatic computer thresholding to ensure that the whole flame was included. Figure 2.11 compares the grayscale and binary images corresponding to an original color photo of a flame.

An average flame image is created using all of the binary flame images. This is performed by simply averaging the intensity value of each pixel over the entire set of images. Because the binary images indicate only flame or no flame with intensity values of 1 and 0 respectively, this image also represents intermittency. The points that are of interest are the locations with pixel intensity values of 0.5, where the flame exists half the time. Values of 0 indicate the flame is never at that location and values of 1 indicate that a portion of the flame always exists at that location, such as near the burner. In practice, there are typically very few points that have an

average intensity value of exactly 0.5, so to provide a larger sample and more defined height area, points with intensity values between 0.48 and 0.52 were selected as the flame height. Points in this intensity range span a vertical distance of approximately 1.5 cm.

The end result of the image processing provides an average image denoting the intermittency of the flame at each pixel, the location of the 50% intermittent points, and the height of these points from the burner indicating the average flame height. To remove the edge effects of the burner on this measurement, only the center third of the burner is used in the height calculation.

Figure 2.12a shows the average image of 380 still photos of the flame. The intensity of each pixel is directly related to the flame intermittency at that location. Pixels that have an intensity value of 0.5 correspond to the flame height and are highlighted in red in Fig. 2.12b. Only the center third of the burner length is used in the calculation, so the 50% intensity points on the edges of the flame are not included in the flame height measurement.

The flame height method described, while it has advantages over visual observer estimates of flame height, does come with a few limitations. These limitations include the fact that the optical recording of the flame only provides a two-dimensional image and is a line-of-sight view of the flame. In the line-fire configuration however, this limitation is believed to have a negligible impact because the camera is positioned to view the long side of the burner and there are limited three-dimensional aspects of the flame by design.

The settings of the camera also could have an influence on the results if the

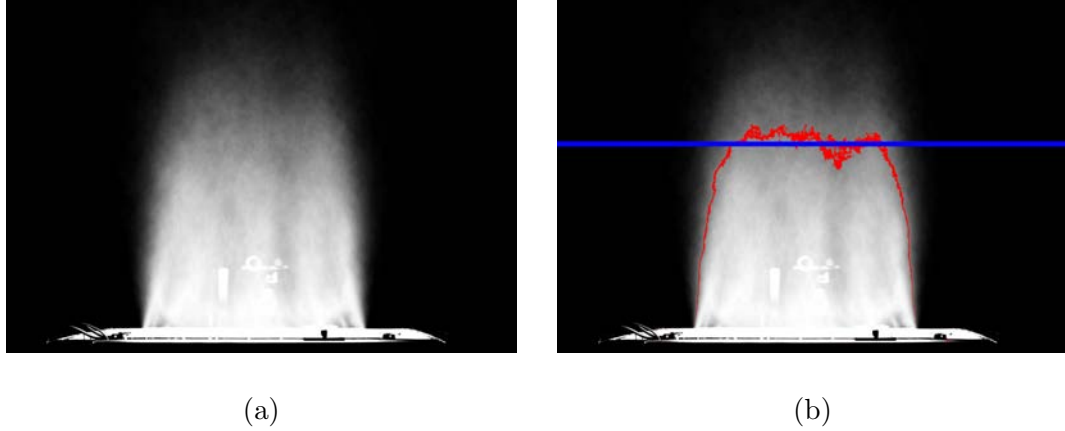


Figure 2.12: The resulting average flame image (a) and flame height identification (b) at 21% O_2 . The 50% intermittent points are marked in red, while the average height is denoted by the blue line.

exposure does not provide distinct contrast on the flame shape. If exposure settings allow over-saturation of the camera sensor, the flame may exhibit a glowing effect, where brightness bleeds into neighboring pixels and reduces the sharp contrast between the flame and background. On the other extreme, if the flame is not bright enough in the image, it becomes difficult to accurately threshold the difference between the flame and background. This difficulty presents itself during suppression experiments where the flame brightness changes dramatically. To avoid this issue of reduced contrast at the edge of the flame, manual control of the camera settings depending on the brightness is adequate. Because the raw color image is eventually converted to a binary image, the amount of saturation in the flame itself is not a concern; the problem only arises when the edge of the flame becomes blurred.

An additional limitation is that this method relies on an average flame measurement and provides limited metrics to statistically evaluate the measurement and

fluctuation of the flame without taking excessively long test samples. Because the flame height measurement comes from 50% intensity points, there is no measure of an instantaneous flame height in individual images of the flame.

2.4.3 Alternate Flame Height Method

An alternate method that also utilizes image processing was investigated to address the limitations related to the average image technique, and to provide a measurement more similar to the one typically done by observation of flame tips. Using the same binary flame images marking the flame location, but without averaging multiple images together, an instantaneous measurement for each flame image can be obtained. For each image, the highest point of the flame in each column of pixels across the image width was located. Averaging the height from each column of pixels yields an instantaneous flame height for any given image of the flame, something that was not possible with the mean flame height method previously described. Figure 2.13 shows a sample image with the top pixels marked in red, and the average height marked by the blue line.

This method does have its own limitations, however. For this calculation, no logic was performed in regard to determining if a small portion of the flame is artificially higher than the bulk of the flame, or if there are dramatic peaks and valleys across the flame that would not indicate the height of the tips accurately. However, this method computes a flame height measurement in the same manner that an observer would do in their mind, without being impaired by judgment.

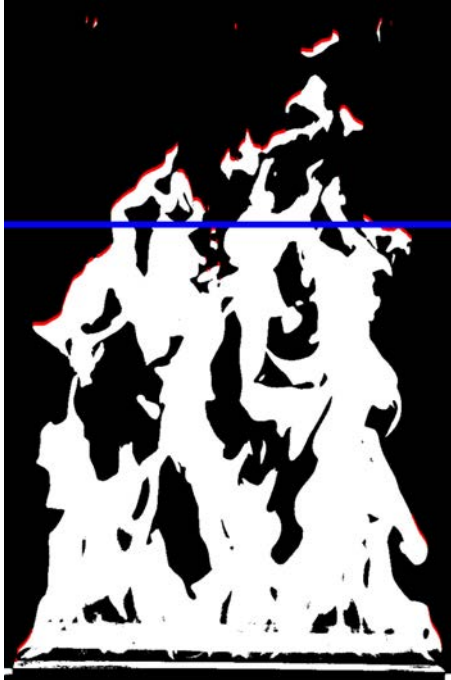


Figure 2.13: Using a single flame image, the highest flame location in each column of pixels is identified (red) and averaged to determine the mean instantaneous flame height, marked by the blue line.

As an additional comparison, estimations of the flame height were made by several observers. This was done by watching a movie playback of a binary image sequence and selecting the location on the image where they believed the average flame height was. A comparison of the results from the different methods is presented in Section 3.2.2.

Chapter 3: Results

3.1 Inlet Measurements

3.1.1 Flow Rate

Flow rate through the co-flow was primarily measured using a pitot tube device in the supply piping upstream of the nitrogen introduction. Calibration of the pitot measurement was done by measuring the oxygen concentration at the co-flow exit during a period when a known amount of nitrogen was supplied to the co-flow stream. The resulting drop in measured oxygen concentration yields the flow rate of fresh room air being supplied to the co-flow. The velocity from the co-flow could then be determined from the bulk flow velocity and the open area at the surface.

Although there is capability to control the co-flow supply using the gate-valve, it was determined that the unrestricted maximum flow rate was the appropriate amount, corresponding to 70 ± 10 g/s (3450 L/min), and a base co-flow velocity of 20 cm/s.

The flow rate of room air through the system remains constant, and the diluent gas is added to this base flow rate. In the case of full suppression, flow rates of nitrogen approached 2400 L/min (14 cm/s), increasing the co-flow velocity to

34 cm/s.

One of the design requirements was that the co-flow velocity be less than one tenth of the buoyant flame velocity. For the 50 kW flame, the estimated buoyant velocity in the flame is on the order of 3.6 m/s, and thus the co-flow velocity meets the design constraint.

3.1.2 Smoke Wire

White smoke generated by heating a mineral oil coated wire provided visualization of the flow to evaluate the uniformity of the co-flow. A sample frame captured from the video, edited to enhance the visibility of the smoke, is shown in Fig. 3.1. To the naked eye the smoke was easily visible, however, viewing on the computer screen required some manipulation to obtain the same contrast and definition of the smoke. Figure 3.1 shows a test with the wire perpendicular to the burner. The portion of the wire situated above the co-flow exit demonstrates a uniform top-hat profile while the portion of the wire outside the co-flow influence displays unstructured smoke generation. The center portion with no smoke is due to the shadow of the burner in the middle of the co-flow.

Visual observations of the smoke indicate the velocity profile of the co-flow is uniform throughout the surface. Lines of smoke rose uniformly if the wire was placed either parallel or perpendicular to the burner. In the perpendicular configuration shown in Fig. 3.1, the smoke rises at the same velocity on both sides of the burner, indicating that either side of the flame is seeing the same co-flow velocities, and

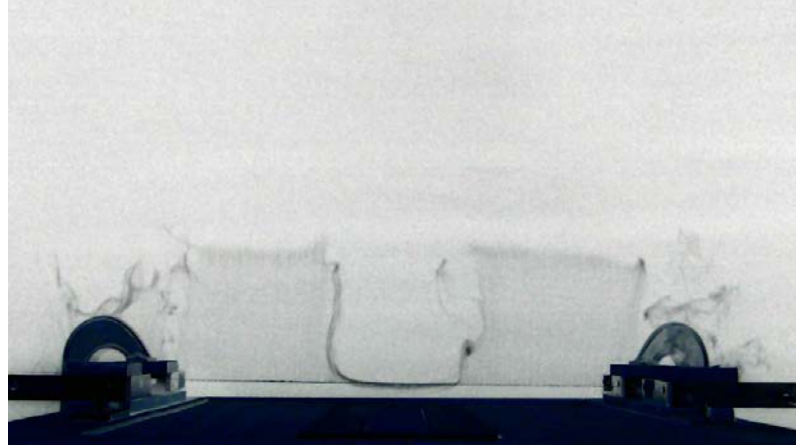


Figure 3.1: A video frame capturing the smoke produced by the heated wire viewed from the short end of the burner. The smoke indicates a uniform flow velocity at the co-flow, and the location of the burner is clearly defined by the area where the smoke does not rise. Outside of the co-flow region, the smoke does not follow any particular path.

therefore the same conditions.

Measurements of the smoke velocity were obtained from the video in an attempt to provide a secondary measurement of the co-flow velocity. The position of the smoke front was recorded for each frame of the video recording and determined the velocity of the flow. Figure 3.2 shows the relationship between the velocity of the smoke front and the velocity of the co-flow from the co-flow, as determined using the bulk volume flow rate. At the zero flow condition, in the absence of the co-flow, it was determined that the velocity of the smoke was on the same order as the air velocity. Therefore, any attempt to get a measure of the air velocity using the smoke has a large error due to the buoyant velocity. The graph in Fig. 3.2 shows that the smoke velocity is not an adequate measure of the true co-flow velocity.

However, the smoke wire diagnostic provided successful results in regard to

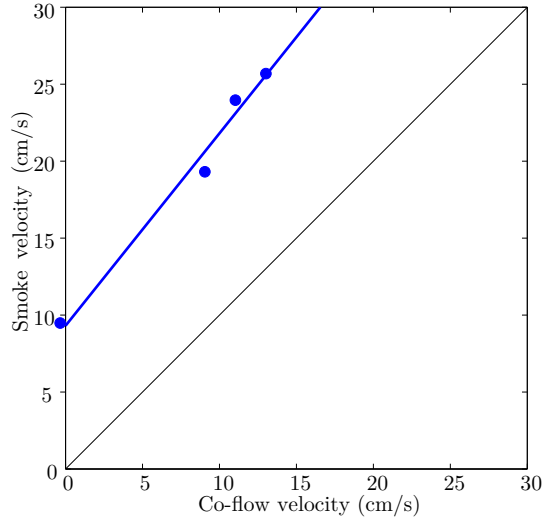


Figure 3.2: Comparison of the flow velocities measured using the smoke-wire technique and the bulk flow rate from the co-flow. The black line indicates a 1:1 correlation.

the evaluation of the co-flow uniformity, the primary objective of the diagnostic. Because the velocity of the smoke is on the same order as the co-flow velocity and is not dominated by the buoyancy, any non-uniformity in the flow would be apparent in the smoke behavior. Because the smoke does not show any influence of velocity gradients when placed at several orientations at the co-flow exit, the velocity from the co-flow is assumed to be constant across the cross-section and directly related to the volumetric flow rate.

3.1.3 Oxygen Concentration

Oxygen concentration measurements at the surface of the co-flow were taken at numerous points across the opening. The steady-state measurements at each location were agreeable and indicate that the air supply is becoming well-mixed

prior to its interaction with the flame. The well-mixed air supply, along with the uniform velocity of the co-flow, means that the flame is interacting with a uniform suppression environment, as desired.

3.2 Flame Measurements

3.2.1 Temperature Profiles

Flame temperature profiles were measured at three heights above the burner—25 cm, 50 cm (nominal flame height), and 75 cm. The 5-minute time-averaged thermocouple measurements are shown in Fig. 3.3 for both the free-burn condition (solid lines) and the co-flow condition (dashed lines).

Based on visual observations, the flame does not appear to be influenced by the co-flow. To support this qualitative observation, temperature profiles of the free-burning flame indicate the burner produces a symmetric peak as desired. Additional temperature profiles measured with the co-flow in operation also produce fairly symmetric behavior that confirms the flame does not tilt dramatically to either side and shows the co-flow does not alter the flame behavior around the axis of the burner. With the co-flow operating, a slight shift in the peak is noticed for the temperature measurements at the 25 and 50 cm heights indicates a very slight tilt. This tilt is approximately 2 cm over a 50 cm height, or 2 degrees. Measurements above the flames at 75 cm show no shift.

Measurements also indicate that the flow straightening honeycomb at the opening of the co-flow help maintain the uniformity of the flame. Temperature measure-

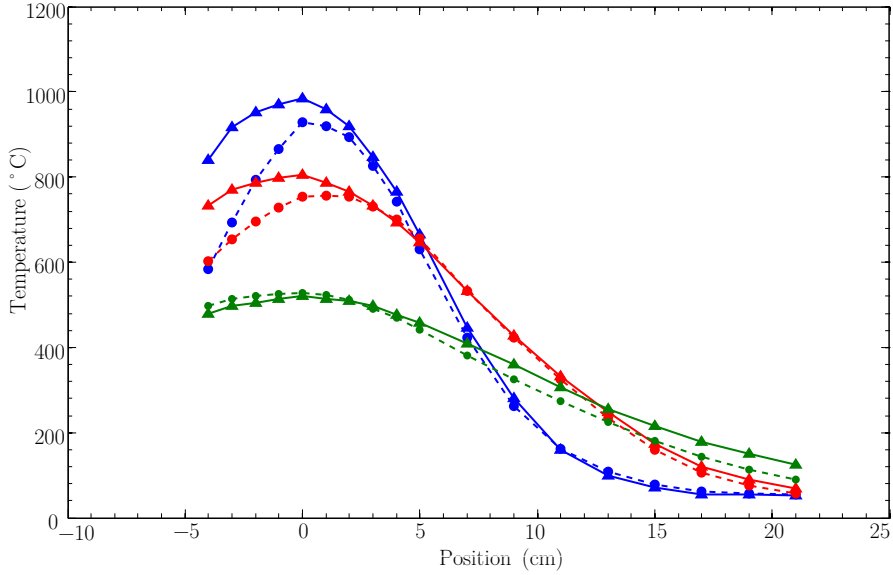


Figure 3.3: Temperature profile measurements obtained at three heights show a symmetric peak at the center of the burner. Additionally, there is good agreement between the measurements taken during a free-burn and with the co-flow operating, indicating that the co-flow does not tilt the flame or alter the temperature. The pairs of lines, from top to bottom are: blue at 75 cm, red at 50 cm, and green at 25 cm heights. The solid lines with triangle points are the free-burn condition, while the dashed lines with circle points are data with the co-flow operating.

ments without the flow straighteners demonstrated a flame tilt of more than 5 cm at a height 75 cm above the burner.

In addition to providing confirmation of the flame shape and consistent temperature between the free-burn and co-flow conditions, the temperature measurements also provide data for CFD model validation. These measurements can be compared to model results of the burner to verify the output of the model to ensure that an unsuppressed flame is being modeled accurately before attempting any suppression modeling.

3.2.2 Flame Height

Various techniques to measure the mean flame height were used to evaluate the design requirement that the flame height be less than the length of the burner, including image analysis methods and visual observations. Results of the different techniques and comparisons to other data are summarized in Table 3.1.

Flame height using the previously described 50% intermittency method with image analysis yields a mean flame height measurement of 0.43 m, which satisfies the design goal that the flame length be no longer than the burner length (0.50 m) to remain a 2-dimensional line flame.

This measured flame height is 20% lower than the 0.54 m measured by Hasemi and Nishihata [15] for a burner with the same 10:1 aspect ratio and heat release rate of 50 kW. It is expected that their measurement is higher because of the visual observer flame-tip method for flame height measurement they used, which would yield a higher result. This is indicated by an estimate of Zukoski [18] that the difference between the two methods lies around 10–15%. This discrepancy in measurements depends heavily on the judgement and definition employed by the observer.

For comparison, the same visual observation method was done by 7 different observers (students in the Fire Protection Engineering Department) on the same flame, and the mean result was 0.50 m, which better relates to the data from both Hasemi and Cox [17]. However, there are significant differences in estimates from observers, ranging from 0.35 m to 0.64 m.

Using an adjusted flame height method, using the highest point of the flame

for each column of pixels in the photo, yields a flame height of 0.49 m. This is a better approximation of the mean flame tip height determined by observers, and also provides instantaneous flame height measurements from individual flame images. For a series of 745 flame images, the instantaneous flame height using the alternative method is presented in Fig. 3.4. The measurement is fairly consistent around the mean value, with a standard deviation of 4.2 cm. The type of flame height fluctuation seen in Fig. 3.4 is expected due to the turbulent nature of the flame, and generally varies within 10 cm of the mean height. Note that the instantaneous flame height measurements are obtained at a nominal rate of 6 Hz and only capture the variations at low frequencies.

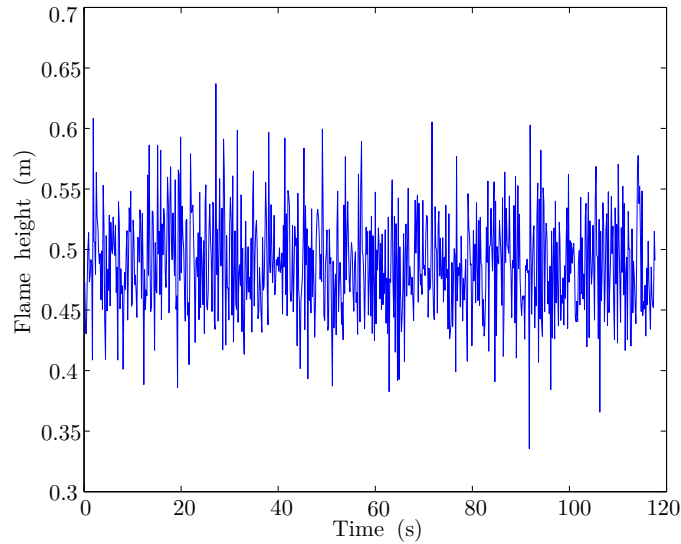


Figure 3.4: The flame height measured using the mean height of the highest point of the flame in each column of pixels across the burner provides a mean flame height of 0.49 cm.

Applied to the dimensionless line heat release rate of the current flame, the correlation to various line fire data sources compiled by Grove [22] suggests a flame

height of 0.45 m, agreeing well with the current measurement method.

Table 3.1: Comparison of flame height measurements using different techniques

Method	Mean Flame Height (m)
50% intermittent	0.43
Highest white pixel	0.49
Visual observation	0.55
Hasemi data [15]	0.54
Grove data fit [22]	0.45
Cox data [17]	0.50

3.3 Suppression Ability

With the addition of nitrogen gas to the co-flow air supply, weakening and complete extinction of the 50 kW methane flame was achieved. The main goal of the co-flow assembly was to construct an experimental facility that was capable of challenging the flame so that detailed suppression measurements could be made in the future. Figure 3.5 shows a sequence of images obtained during the suppression of the methane flame with increasing amounts of nitrogen diluent added to the co-flow supply. The photos were each captured with the same camera settings, and the changes in flame shape, luminous intensity, and color are all evident in this figure.



Figure 3.5: Images showing flame behavior during an experiment where the nitrogen flow rate is slowly increased through the test until the flame is extinguished. Camera settings are identical for each image.

Chapter 4: Conclusions and Future Work

The development of this experimental apparatus provides a well-characterized flame and environment with which to study flame suppression. The flame produced by the burner meets the design requirements that the flame be buoyancy dominated, turbulent, and in a line fire configuration. Measurements and observations of the flame indicate that the surrounding co-flow does not alter the flame shape or behavior.

The buoyancy constraint for the 50 kW methane flame is met, providing a Q^* of 8.12, which is less than the value of 10 desired to be in the buoyant regime. To ensure the line fire configuration, the height of the flame was required to be less than the length of the burner. A robust method to analyze images of the flame was

developed to repeatably determine the height of the flame, and confirmed the design criterion was met with a flame height less than 50 cm.

Oxygen concentration measurements and smoke wire diagnostics of the co-flow system confirm that the co-flow is providing an air flow of four times the stoichiometric combustion requirement for the flame as the design requirements specified. This co-flow supply is confirmed to be uniform in both oxygen concentration and velocity distribution across the opening. Temperature measurements of the flame show that there is no change in flame tilt or temperature in the flame when the co-flow is operational, indicating that the co-flow does not influence the flame other than the intended change in oxygen concentration.

The careful consideration given to the inlet conditions provides friendly boundary conditions to utilize in computer models to simulate the suppression experiments conducted with this apparatus and validate the models with the experimental results.

Addition of an inert diluent to the co-flow oxidizer stream successfully challenges the flame to extinction. In the future, water mist nozzles will be added to the co-flow box to present another challenge to the flame rather than inert gas. Additionally, the design of the burner easily permits the use of additional fuels such as propane in the future. To gain a deeper understanding of suppression efforts on the flame, calorimetry is proposed to measure combustion efficiency from partially suppressed flames.

Bibliography

- [1] R.R. Simmons and H.G. Wolfhard. Some limiting oxygen concentrations for diffusion flames in air diluted with nitrogen. *Combustion and Flame*, 1:155–161, 1957.
- [2] R. Hirst and K. Booth. Measurement of flame-extinguishing concentrations. *Fire Technology*, 13(3):296–315, 1977.
- [3] S. Ishizuka and H. Tsuji. An experimental study of effect of inert gases on extinction of laminar diffusion flames. In *Eighteenth Symposium (International) on Combustion*, pages 695–703. The Combustion Institute, 1981.
- [4] J. Suh and A. Atreya. The effect of water vapor on counterflow diffusion flames. In *International Conference on Fire Research and Engineering*, pages 103–108, 1995.
- [5] E.A. Ural. Measurement of the extinguishing concentration of gaseous fuels using the cup-burner apparatus. In *Halon Options Technical Working Conference*, pages 275–283, 1999.
- [6] B.T. Fisher, A.R. Awtry, R.S. Sheinson, and J.W. Fleming. Flow behavior impact on the suppression effectiveness of sub-10- μm drops in propane/air co-flow non-premixed flames. In *Proceedings of the Combustion Institute 31*, pages 2731–2739. The Combustion Institute, 2007.
- [7] W.M. Pitts, R.A. Bryant, and J.C. Yang. Thermal agent extinguishment of two types of diffusion flames. In *Second Joint Meeting of the United States Sections of the Combustion Institute*, 2001.
- [8] I.K. Puri and K. Seshadri. Extinction of diffusion flames burning diluted methane and diluted propane in diluted air. *Combustion and Flame*, 65:137–150, 1986.
- [9] C.C. Ndubizu, R. Ananth, P. Tatem, and V. Motevalli. On water mist fire suppression mechanisms in a gaseous diffusion flame. *Fire Safety Journal*, 31:253–276, 1998.

- [10] A. Atreya, T. Crompton, and J. Suh. A study of the chemical and physical mechanisms of fire suppression by water. In *Fire Safety Science—Proceedings of the Sixth International Symposium*, pages 493–504. International Association for Fire Safety Science, 1999.
- [11] A.K. Lazzarini, R.H. Krauss, H.K. Chelliah, and G.T. Linteris. Extinction conditions of non-premixed flames with fine droplets of water and water/NaOH solutions. In *Proceedings of the Combustion Institute 28*, pages 2939–2945. The Combustion Institute, 2000.
- [12] H. Tsuji and I. Yamaoka. The counterflow diffusion flame in the forward stagnation region of a porous cylinder. In *Eleventh Symposium (International) on Combustion*, pages 979–984. The Combustion Institute, 1967.
- [13] NFPA 2001: Standard on clean agent fire extinguishing systems, 2012.
- [14] R.J. Santoro, H.G. Semerjian, and R.A. Dobbins. Soot particle measurements in diffusion flames. *Combustion and Flame*, 51:203–218, 1983.
- [15] Y. Hasemi and M. Nishihata. Fuel shape effect on the deterministic properties of turbulent diffusion flames. In *Fire Safety Science—Proceedings of the Second International Symposium*, pages 275–284. International Association for Fire Safety Science, 1989.
- [16] O. Sugawa, Y. Oka, and H. Satoh. Flame height from rectangular fire sources considering mixing factor. In *Fire Safety Science—Proceedings of the Third International Symposium*, pages 435–444. International Association for Fire Safety Science, 1991.
- [17] L. Yuan and G. Cox. An experimental study of some line fires. *Fire Safety Journal*, 27:123–139, 1996.
- [18] E.E. Zukoski, B.M. Cetegen, and T. Kubota. Visible structure of buoyant diffusion flames. In *Twentieth Symposium (International) on Combustion*, pages 361–366. The Combustion Institute, 1984.
- [19] L. Audouin, G. Kolb, J.L. Torero, and J.M. Most. Average centreline temperatures of a buoyant pool fire obtained by image processing of video recordings. *Fire Safety Journal*, 24:167–187, 1995.
- [20] B. Karlsson and J.G. Quintiere. *Enclosure Fire Dynamics*. CRC Press LLC, Boca Raton, FL, 2000.
- [21] C.L. Beyler. Fire plumes and ceiling jets. *Fire Safety Journal*, 11:53–75, 1986.
- [22] B.S. Grove and J.G. Quintiere. Calculating entrainment and flame height in fire plumes of axisymmetric and infinite line geometries. *Journal of Fire Protection Engineering*, 12:117–137, 2002.

- [23] J. White. Dissertation proposal: Suppression of a buoyant, turbulent line flame via oxidizer-dilution or water-mist: Experiment and LES. University of Maryland, 2014.
- [24] L. I. Gaby. Hot-wire smoke streams for visualization of air flow patterns. *J. Sci. Instrum.*, 43:334, 1966.
- [25] T. Jin. Visibility and human behavior in fire smoke. In *SFPE Handbook of Fire Protection Engineering*. National Fire Protection Association, 3rd edition, 2002.